

Model system for investigating laser-induced subcellular microeffects

Gereon Hüttmann, Jesper Serbin, Benno Radt, Björn I. Lange and Reginald Birngruber
Medical Laser Center Lübeck, Peter-Monnik-Weg 4, D-23562 Lübeck, Germany

ABSTRACT

Background: Laser induced protein denaturation is of fundamental interest for understanding the mechanisms of laser tissue interaction. Conjugates of nanoabsorbers coupled to proteins are presented as a model system for investigating ultrafast protein denaturation. Irradiation of the conjugates using repetitive picosecond laser pulses, which are only absorbed by the nanoabsorbers, could result in effects with a spatial confinement of less than 100 nm.

Materials and Methods: Experiments were done with bovine intestinal alkaline phosphatase (aP) coupled to 15 nm colloidal gold. This complex was irradiated at 527 nm wavelength and 35 ps pulse width with a varying number of pulses ranging from one up to 10^4 . The radiant exposure per pulse was varied from 2 mJ/cm^2 to 50 mJ/cm^2 . Denaturation was detected as a loss of protein function with the help of the fluorescence substrate 4MUP.

Results and Discussion: Irradiation did result in a steady decrease of the aP activity with increasing radiant exposures and increasing number of pulses. A maximal inactivation of 80% was reached with 10^4 pulses and 50 mJ/cm^2 per pulse. The temperature in the particles and the surrounding water was calculated using Mie's formulas for the absorption of the nanometer gold particles and an analytical solution of the equations for heat diffusion. With 50 mJ/cm^2 , the particles are heated above the melting point of gold. Since the temperature calculations strongly depend on changes in the state of matter of the particles and water, a very sophisticated thermal model is necessary to calculate exact temperatures.

It is difficult to identify one of the possible mechanisms, thermal denaturation, photochemical denaturation or formation of micro bubbles from the dependance of the inactivation on pulse energy and number of applied pulses. Therefore, experiments are needed to further elucidate the damage mechanisms.

In conclusion, denaturing proteins irreversibly via nanoabsorbers using picosecond laser pulses is possible. The confinement of the heat to the nanoabsorbers when irradiating with picosecond pulses suggests that the denaturation of proteins could be possible with nanometer precision in cells with this approach. However, the mechanism of protein inactivation, which is part of present investigations, is crucial for the precision of such nanoeffects.

Keywords: Laser medicine, nanoparticles, colloidal gold, protein denaturation

1. INTRODUCTION

Lasers are used in a large variety of medical applications because of their ability to modify or destroy tissue with high precision. Two different ways may be used to restrict the laser-induced damage to the target volume. The laser beam can either be focused directly to the target tissue, or a selective absorption in the tissue can be used to restrict damage to the target volume (Fig. 1). When focusing the laser beam, the precision of the laser induced effects is limited by the size of the laser focus, which can be in the order of a micron, if optics with a high numerical aperture are used.^{1,2} For applications in real tissues even this precision may not be achieved. Typical examples for this kind of laser application are laser cutting or laser ablation. Using differences in tissue absorption, the temperature can be raised selectively in the stronger absorbing structures. These high temperatures give the opportunity for a destruction of the absorbing structures. The precision of these effects can be comparable to the size of the absorber,

Further author information: (Send correspondence to Gereon Hüttmann)

Gereon Hüttmann: E-mail: huettmann@mll.mu-luebeck.de

Benno Radt: E-mail: radt@mll.mu-luebeck.de

Jesper Serbin: E-mail: js@lzh.de

Brörn I. Lange: E-mail: lange@mll.mu-luebeck.de

Reginald Birngruber: E-mail: bgb@mll.mu-luebeck.de

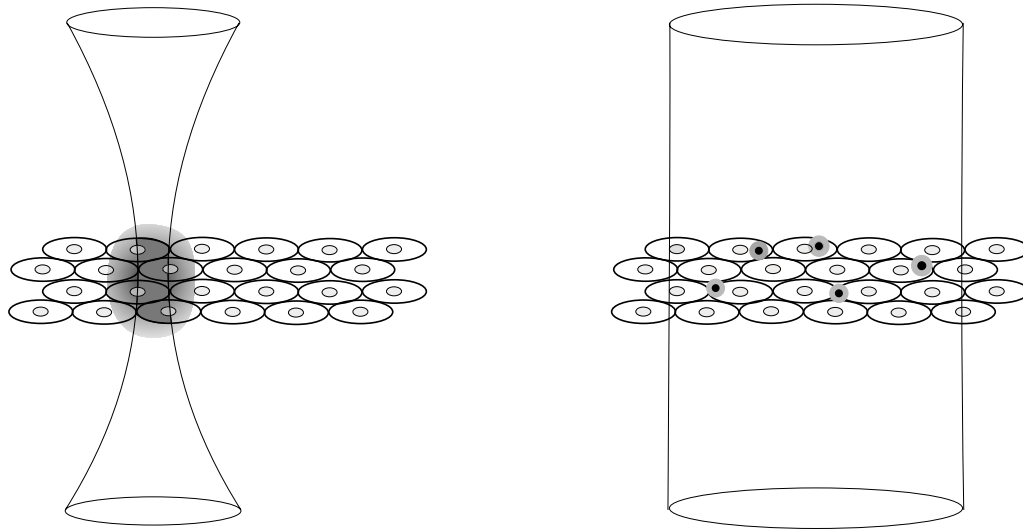


Figure 1. Localized tissue damage can be induced either by tight focusing of the laser beam (left) or by using increased absorption in the target structures (right).

if the collateral damage, caused by heat diffusion, shock-waves, or mechanical destruction can be limited to the near vicinity of the absorbing structures. In order to limit heat diffusion, the pulse width of the laser irradiation has to be shorter than the thermal relaxation time of the heated volume. This principle of high precision laser effects, which was proposed by Parrish and Anderson,³ is often called selective thermolysis. Several clinical applications of lasers rely on this principle, e. g. laser epilation,⁴ the phototherapy of port wine stains with pulsed lasers,^{5,6} or the selective photocoagulation of the retinal pigment epithelium with microsecond laser pulses⁷ in which single melanin containing cells can be destroyed selectively.

At the moment it is not clear whether also cell organelles or even single macromolecules like proteins or DNA can be selectively destroyed by photothermolysis. The generation of high temperatures in nanometer volumes is possible since strongly absorbing particles, which can create temperatures of several thousand Kelvins on their surface, are available with diameters in the nanometer range. The main problem, when going to smaller structures, is the reduction of the laser pulse width, which is necessary to stay in the thermal confinement. This decreases the duration of increased temperature in the tissue. Since thermal damage depends on temperature and time,^{8,9} the reduction in time has to be compensated for by an increased temperature. A high temperature and a very fast temperature increase can cause mechanical disruption by evaporation of water or shock waves, which may then destroy the precision of the laser-induced effects. Since thermal damage for multiple temperature expositions adds up, the necessary peak temperature can be reduced using multiple pulses. The additivity of laser induced damage was shown in a large variety of experiments, e. g. laser induced damage of the retina^{10,11} or thermal damage of vascular tissue.¹² Extrapolation of rates of thermal damage of proteins and tissues to very high temperatures shows the possibility of selective thermal damage of biological structures near strongly absorbing nanometer-sized particles.¹³

Several groups have investigated the possibility of sub-cellular thermal damage. Jori et al. postulated the possibility of using single strongly absorbing molecules to create thermal damage in cells.¹⁴ In this work, however, the increase of the damage temperature with decreasing heating time was not taken into account. If this is considered, molecules will rather undergo photochemistry than cause a sufficient temperature increase, as calculations have shown.¹³ This was also supported by experiments in which malachite green was used to inactivate proteins under irradiation with nanosecond laser pulses.¹⁵ Although these experiments were designed for a thermal inactivation, it was later shown that radical formation destroyed the proteins.¹⁶ In recent experiments, phototoxic effects of Cu(II)-hematoporphyrin and a Ni(II)-naphthalocyanine were observed in cell culture and tumor bearing mice, when irradiated with Q-switched pulses.^{17,18} The observations that the substances do not produce singlet oxygen and that with cw irradiation no cytotoxic effects were observed, led to the supposition of photothermal damage of the cells under nanosecond irradiation.

The aim of this work was to investigate the possibility of protein inactivation on an ultrashort time scale by the irradiation of protein-gold conjugates with picosecond laser pulses. For the experiments, conjugates made of colloidal gold with a diameter of 15 nm and alkaline phosphatase (aP) were chosen, because they were commercially available. Alkaline phosphatase is commonly used for a variety of enzymatic assays, and therefore simple and sensitive assays for probing its activity exist. These conjugates were irradiated with a mode-locked frequency-doubled Nd:YLF laser. After irradiation the residual activity of the proteins was measured by a fluorescence assay.

2. MATERIALS AND METHODS

2.1. Samples and measurement of the protein activity

The conjugates of 15 nm gold particles with bovine intestinal alkaline phosphatase were purchased from ICN Biomedical Inc. Although the conjugates can be stored at 4°C for several weeks, a certain amount of proteins separates from the gold particles during storage, because the proteins are not covalently bound to the particle surface. Therefore, in the beginning of each experiment, unbound proteins were removed by centrifugation at 10000 rpm for 45 min. The loose pellet was carefully transferred with a pipette to a new vial, where they were resuspended in phosphate buffer. After this procedure the aP activity of unbound protein was less than 25% of the activity of the aP-gold conjugates. Additionally, the activity of the bound and free aP was measured before and after irradiation.

The activity of aP was measured with 4-MUP (4-Methylumbelliferylphosphatase, Calbiochem), which was used in a concentration of 10 mMol/l in DEA (Diethanolamine, Fluka). Through cleavage of the phosphate group from 4-MUP, a new derivative of the dye (4-MU) is produced, which fluorescence excitation/emission maxima are shifted from 323 nm/385 nm to 370 nm/445 nm. The aP-activity was measured in 2 mm wells with a fluorescence spectrometer (Fluoromax, Spex), which was equipped with a quartz fiber bundle in order to transmit excitation and fluorescence light between the spectrometer and the samples, which were excited at 370 nm. The fluorescence was measured at 445 nm. Since at these wavelength the fluorescence of 4-MUP is very small a conversion of 4-MUP to 4-MU through the catalytic action of aP results in an increase of the measured fluorescence signal with time. Using different concentrations of aP, it was checked that under our experimental conditions the slope of the fluorescence increase was in a linear relationship to the concentration of active aP.

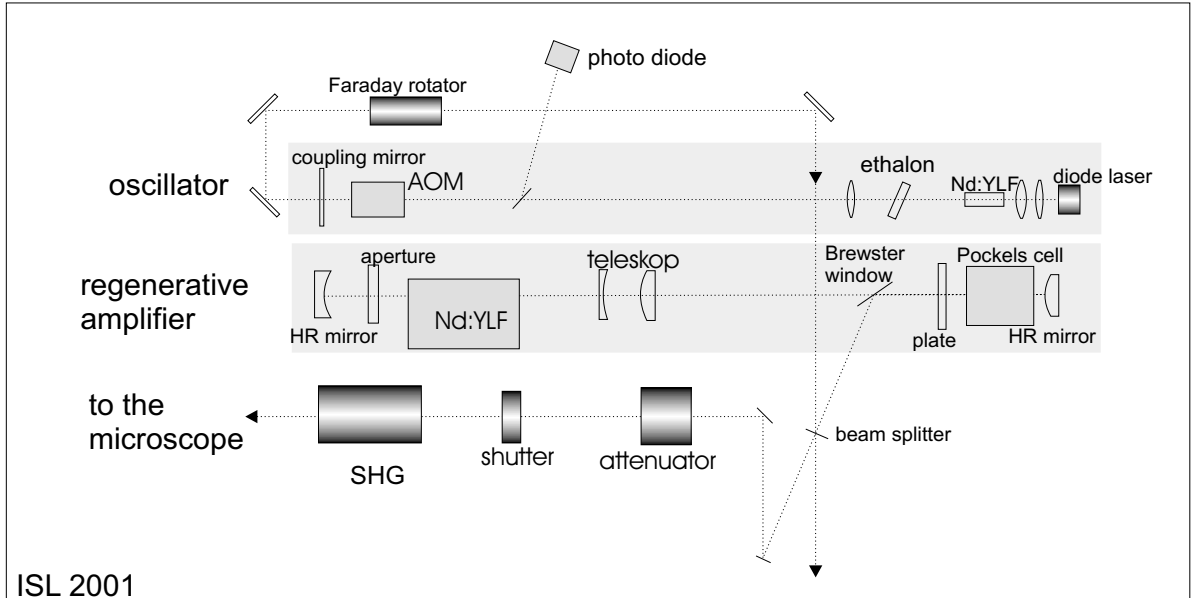
2.2. Irradiation of the samples

The samples were irradiated with a mode-locked Nd:YLF laser (ISL 2001 MPL, Intelligent Laser Systems Inc.) which was originally build for ophthalmic laser applications, but then modified for these experiments. The system consists of a cw pumped oscillator, which generates a continuous train of picosecond pulses with 167 MHz repetition rate, and a regenerative amplifier (Fig. 2a). The oscillator, which is actively mode-locked by an acousto-optic modulator, emits at a wavelength of 1057 nm. After passing a Faraday rotator, a small fraction of the picosecond pulses were fed into the amplifier. With an Electro-Optic Pockels cell a single picosecond pulse is selected, which is then amplified in the cavity of the regenerative amplifier in approximately 100 round trips. When the inversion in the active medium is depleted, the Pockels cell is switched again and the pulse is ejected from the cavity. The amplifier can generate pulses with an energy of up to 1 mJ at a rate of 1 kHz. Due to the high quality of the cavity and the large number of round trips in the regenerative amplifier, a large amplification factor in the order of 10^6 can be achieved even though the active medium is pumped only by an cw arc-lamp. The large number of round trips also gives a very good discrimination against higher transverse modes. This and the low pump intensity compared to a flash lamp pumped system give a stable output energy with 5% standard deviation together with a Gaussian intensity distribution.¹⁹

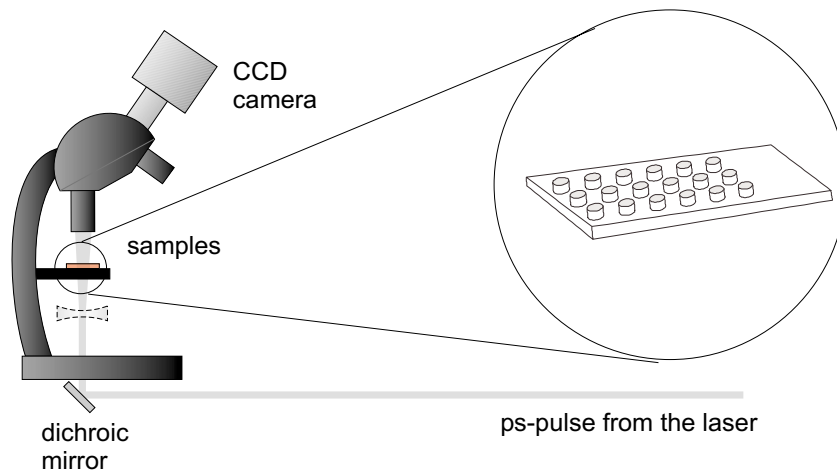
With a $\lambda/2$ -plate and a polarizer, the pulse energy can be attenuated to the desired level. A 15 mm LBO crystal (Casix) was used for frequency doubling of the infra-red radiation. LBO was chosen because of its high damage threshold and the possibility of non-critical phase matching. The resulting large acceptance angle allows an efficient doubling even with slightly divergent beams. The crystal was heated in an self-built oven to 167°C. With a slight focusing of the output beam, a doubling efficiency of over 40% was achieved.

The pulse width of the oscillator was measured with a self-built autocorrelator using an Michelson interferometer and a 4 mm LBO crystal. The full width at half maximum of the autocorrelation trace was 75 ps. Assuming a Gaussian pulse profile, the pulse width can be estimated to 53 ps. During the frequency doubling the pulse is shortened by a factor of $\sqrt{2}$. Therefore, at 527 nm the pulse width was around 35 ps.

The samples were irradiated in wells with a diameter of 2 mm, which were custom-made in a 25 mm x 75 mm slide of optical glass (Hellma). Each of the 18 wells took a sample volume of 3.5 μ l. The glass slide was positioned under a



a)



b)

Figure 2. Set-up for the irradiation of the aP-gold conjugates. a) Mode-locked frequency-doubled Nd:YLF-laser, which generated the picosecond pulses b) Microscope, which was used for positioning of the samples during the irradiation.

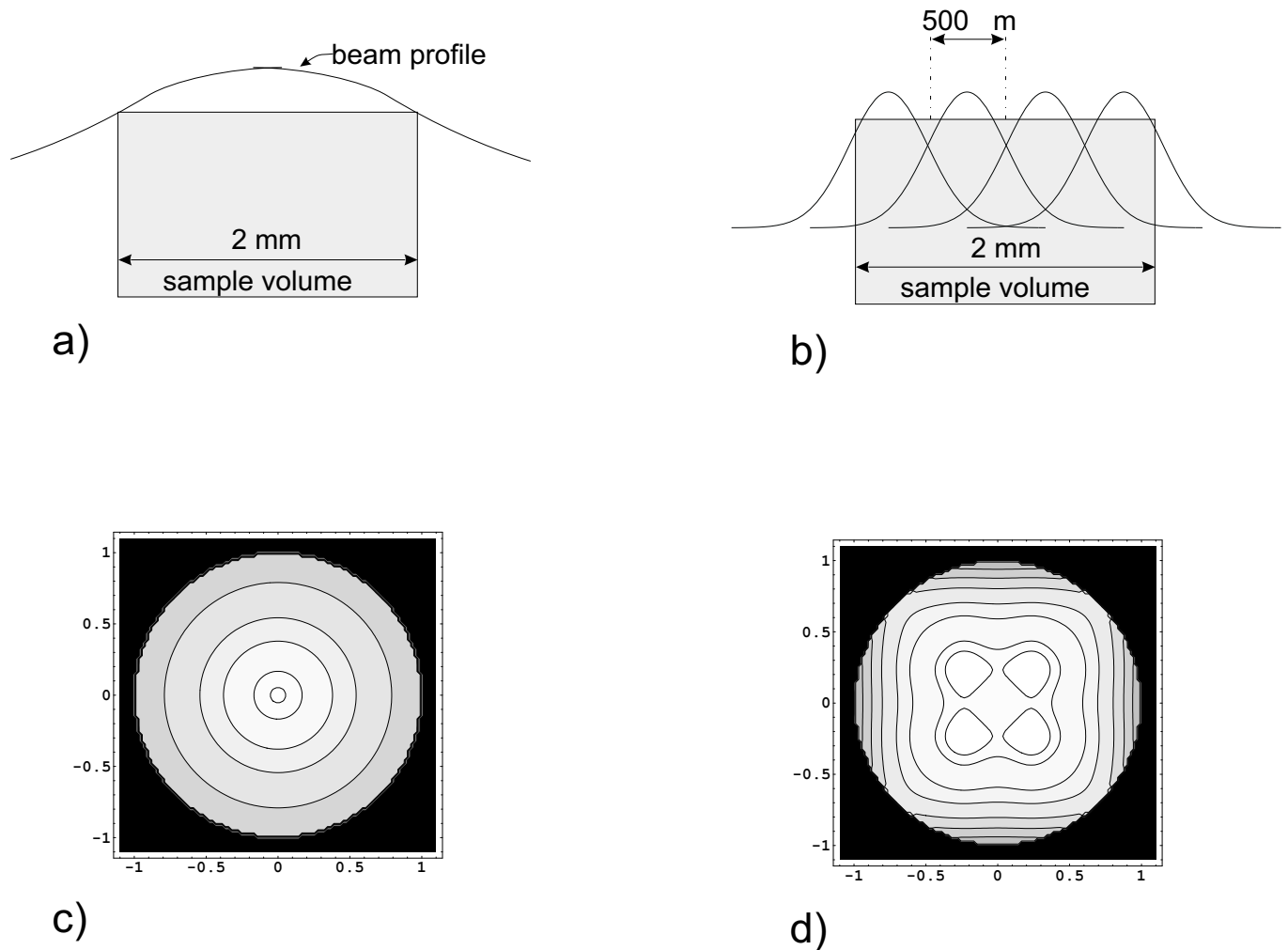


Figure 3. Distribution of the radiant exposure inside the sample volume. a), c) Irradiation with the expanded beam. b), d) Scanned irradiation with a 0.5 mm beam. c) and d) show a contour plot of the total radiant exposure. The contour lines were drawn at 50%, 60%, 70%, 80%, 90%, 95%, 99%, and 99.9% of the maximum.

microscope, the illumination system of which was replaced by a dichroic mirror in order to guide the irradiation beam to the sample and separate frequency-doubled light from the infrared irradiation (Fig. 2b). For the irradiation, the laser beam was either expanded using a diverging lens or the unexpanded laser beam was scanned over the sample area. In the first case, 30% of the beam passed through a 2 mm aperture, which means that, assuming a gaussian beam profile, the irradiance at the rim of the 2 mm samples was 70% of the maximal irradiance in the center (Fig. 3a and b). The radiant exposure averaged over the area of 2 mm was 2 mJ/cm² at maximal pulse energy. In order to achieve a higher exposure, the unexpanded beam, which had a diameter of approximately 0.5 mm, was directed to a field of 4x4 spots in the sample, which had a distance of 0.5 mm from each other (Fig. 3b). With this approach, a nearly homogeneous total radiant exposure of up to 50 mJ/cm² per pulse was achieved (Fig. 3d). The average radiant exposure was measured by either placing a 2 mm or a 0.5 mm aperture in front of a pyroelectric energy meter (PE10, Ophir). The radiant exposure was then calculated by dividing the measured pulse energy by the area of the aperture.

2.3. Temperature calculations

The temperature at the surface and in the surroundings of gold particles in water was calculated using Mie's formula for the efficiency factor of absorption Q_{abs} and an analytical solution of the differential equations for heat diffusion. For 15 nm particles, which are small compared to the wavelength, the ratio of the absorption cross-section and the geometric cross-section of the particle (Q_{abs}) can be calculated with an accuracy of a few percent by a simple approximation²⁰:

$$Q_{abs} = -\frac{8\pi R}{\lambda} \text{Im} \left(\frac{m^2 - 1}{m^2 + 2} \right). \quad (1)$$

λ is the wavelength of the irradiating light in water, R the radius of the particle. m , which is the index of refraction of gold divided by that of the surrounding water, was taken as $0.59 - i 1.67$.²⁰ With Equation (1), the power density A of absorbed light inside a particle, which is irradiated with the irradiance I , can be calculated:

$$A = I \frac{Q_{abs} \pi R^2}{4/3 \pi R^3}. \quad (2)$$

During the irradiation, part of the thermal energy diffuses into the water. This was accounted for with help of a solution for the differential equations for macroscopic heat diffusion which describes the temperature in and around a sphere, that is embedded in an infinite medium. In this solution, it is assumed that starting at time zero heat is produced homogeneously with a rate A inside of the particle.²¹ Thermal conductivity K and thermal diffusivity κ in the sphere can differ from the respective values of the surrounding medium. At the surface, a steady change of the temperature is assumed when passing from inside to outside. With these assumptions, the temperature inside (T_1) and outside (T_2) the particle can be calculated from following formulas:

$$T_1(t, r) = \frac{R^2 A}{K_1} \left[\frac{1}{3} \frac{K_1}{K_2} + \frac{1}{6} \left(1 - \frac{r^2}{R^2} \right) - \frac{2Rb}{r\pi} \cdot \int_0^\infty \frac{\exp\left(-\frac{y^2 t}{\gamma_1}\right)}{y^2} \frac{(\sin y - y \cos y) \sin\left(\frac{ry}{R}\right)}{\left[(c \sin y - y \cos y)^2 + b^2 y^2 \sin^2 y \right]} dy \right] \quad (3)$$

$$T_2(t, r) = \frac{R^3 A}{rK_1} \left[\frac{1}{3} \frac{K_1}{K_2} - \frac{2}{\pi} \int_0^\infty \frac{e^{-\frac{y^2 t}{\gamma_1}}}{y^3} \frac{(\sin y - y \cos y) [by \sin y \cos \sigma y - (c \sin y - y \cos y) \sin \sigma y]}{\left[(c \sin y - y \cos y)^2 + b^2 y^2 \sin^2 y \right]} dy \right] \quad (4)$$

with

$$b = \frac{K_2}{K_1} \sqrt{\frac{\kappa_1}{\kappa_2}}, \quad c = 1 - \frac{K_2}{K_1}, \quad \sigma = \left(\frac{r}{R} - 1 \right) \sqrt{\frac{\kappa_1}{\kappa_2}}, \quad \gamma_1 = \frac{R^2}{\kappa_1}.$$

The parameters inside the sphere are denoted by the suffix 1, the parameters of the medium by suffix 2.

Equations (3) and (4) give the time-dependent temperature for an unlimited long pulse. Since the differential equations for heat diffusion are linear in time, a solution for a rectangular laser pulse with the pulse width τ can be constructed by subtracting two solution $T(t, r)$, which are separated in time²²:

$$T_{\square}(t, r) = T(r, t) - T(r, t - \tau) \quad (5)$$

3. RESULTS

3.1. Irradiation of the conjugates

With the expanded beam, no inactivation of the irradiated aP-gold conjugates was observed, even when the samples were irradiated with 10^4 pulses. As an example, Fig. 4a shows the increase of the 4-MU fluorescence of ten samples, of which five were irradiated with 10^4 pulses at 2.1 mJ/cm^2 . From the fluorescence intensity of each sample, the slope was calculated, which is proportional to the activity of the aP in the samples (Fig. 4b). No significant reduction of the aP activity after irradiation was observed at that radiant exposure. When a higher radiant exposure was used

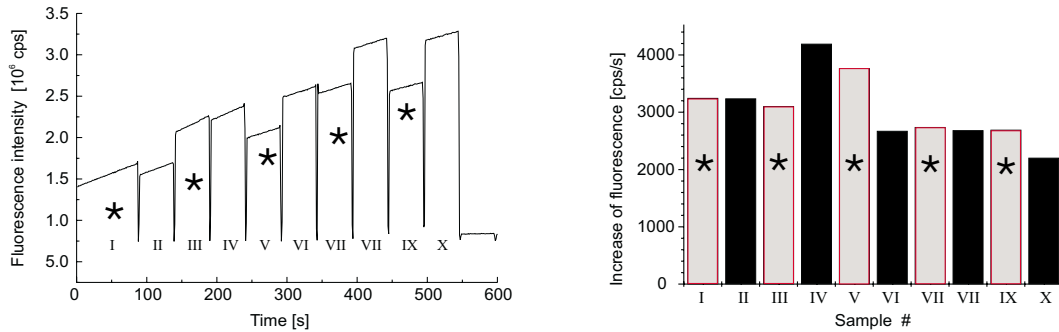


Figure 4. Activity of alkaline phosphatase after irradiation with 10^4 pulses at 2.1 mJ/cm^2 .
 a) 4-MU fluorescence of ten samples measured over 70 s. Only five samples marked by a star (*), were irradiated; the other non-irradiated samples served as a control.
 b) Slope of the fluorescence of the tens samples, which is proportional to the aP activity.

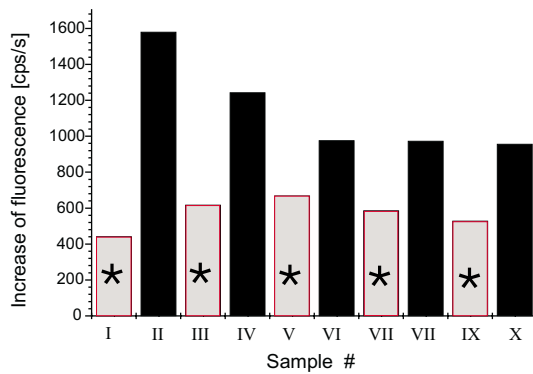


Figure 5. Activity of aP after irradiation with 16×10^4 pulses at 50 mJ/cm^2 . Irradiated samples are marked by a star (*), the remaining samples are controls.

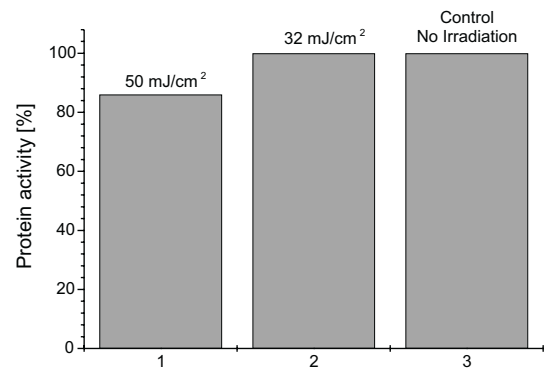


Figure 6. Activity of uncoupled alkaline phosphatase in solution, after irradiation with 10^4 pulses at different radiant exposure.

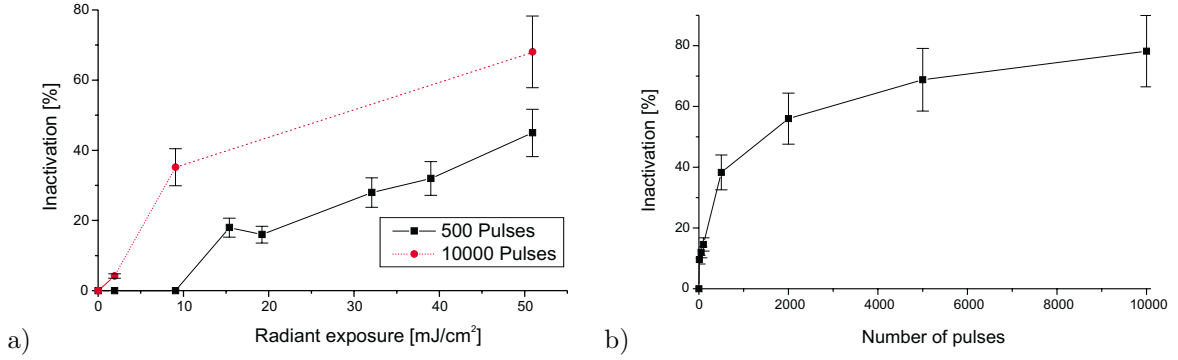


Figure 7. Inactivation of aP bound to the gold particles.

a) Dependence of the inactivation on the radiant exposure for 500 and 10^4 pulses.

b) Dependence of the inactivation on the number of pulses at a radiant exposure of 50 mJ/cm^2 .

by scanning the sample with the 0.5 mm laser beam in 16 fields, the activity of the aP in the samples was markedly reduced (Fig. 5). When in a control experiment a solution of unbound alkaline Phosphatase was irradiated under the same conditions, only a slight reduction of the aP activity was observed (Fig. 6).

The inactivation of aP (IA) was defined by the loss of activity due to the irradiation divided by the protein activity without irradiation:

$$IA = \frac{A_{Con} - A_{Irr}}{A_{Con}} \quad (6)$$

A_{Con} and A_{Irr} are the slopes of the 4-MU fluorescence of control samples which were not irradiated, and the irradiated samples, respectively. Even though unbound aP was removed from the samples before irradiation by centrifugation, there was always a certain amount of unbound protein in the sample, that could not be inactivated by the picosecond irradiation. In order to correct the measured inactivation for this error, a fraction of the sample solution was spun down before the experiments were conducted, and the activity of the sediment A_{Sed} and the supernatant A_{Sup} were measured. The inactivation IA was then corrected by the factor $(A_{Sed} - A_{Sup})/A_{Sed}$.

Protein activity was measured for different radiant exposures and different numbers of pulses and the corrected inactivation was calculated from these measurements. With single pulses, no inactivation was observed up to a radiant exposure of 50 mJ/cm^2 . With 500 pulses, the protein activity was reduced with a radiant exposure above 10 mJ/cm^2 (Fig. 7a). After irradiation with 50 mJ/cm^2 , proteins were inactivated by nearly 40%. After an irradiation with 10^4 pulses the effect was even stronger. 10 mJ/cm^2 gave nearly 40% inactivation, and with 50 mJ/cm^2 the activity was reduced by almost 70%. The dependance of the inactivation on the number of pulses was measured for 50 mJ/cm^2 (Fig. 7b).

3.2. Temperature calculation

The temperature distribution inside and in the surroundings of a 15 nm gold particle immersed in water was calculated for a 50 ps rectangular laser pulse at different times after the beginning of the pulse (Fig. 8). Since the thermal diffusivity of gold is nearly 900 times larger than that of water, the temperature inside the particle stays constant across the radius during the cooling: The temperature in the center exceeds the temperature at the rim only by a few percent. In contrast, the temperature decreases quite rapidly in the surrounding of the particle. At the distance of 10 nm from the particle surface, the temperature reaches less than 5% of the temperature of the surface. 10 nm is the approximate size of aP, which is bound to the surface of the gold particles. Therefore, a strong temperature gradient along the proteins is expected. After the end of the laser pulse, the particle rapidly cools down within hundreds of picoseconds (Fig. 8b). 400 ps after the beginning of the pulse the surface has only 10% of the maximal temperature which is reached at the end of the pulse.

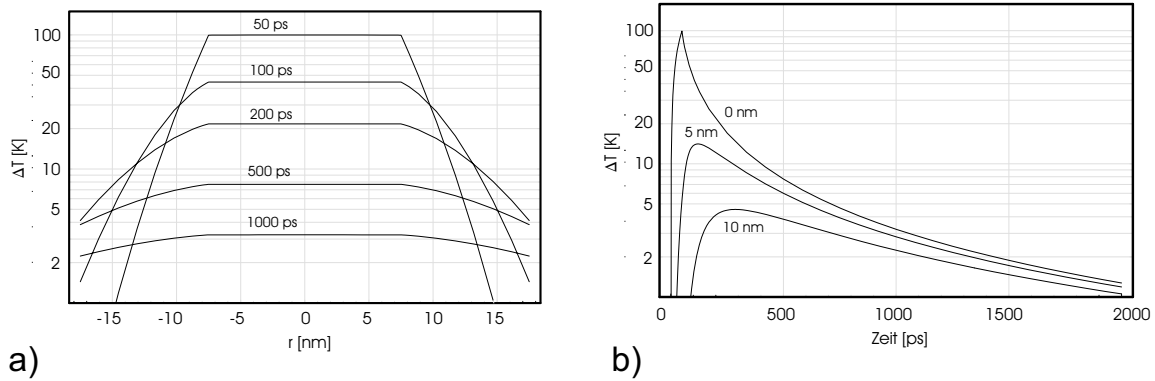


Figure 8. a) Temperature distribution inside and around a 15 nm gold particle when irradiated with 1 mJ/cm^2 at various times after the beginning of the irradiation. b) Change of the temperature with time at the surface, in 5 nm and 10 nm distance from the surface.

4. DISCUSSION

Aim of these experiments was to investigate whether it is possible to inactivate proteins which are bound to nanometer-sized gold particles by picosecond laser irradiation. Ultra short pulses were used in order to prevent heat diffusion to the surrounding water. Due to the high absorption of the gold particles, extremely high temperatures can be reached at the surface of the particles with pulses of 50 ps width. The temperature is increased by approximately 100 K with every mJ/cm^2 radiant exposure. These temperatures are localized in a volume with a diameter of 35 nm and last only a few hundred picoseconds. Under these conditions, a reduction of the activity of proteins which were bound to the gold particles was observed, when the samples were irradiated with multiple pulses. With 500 pulses, inactivation started above 10 mJ/cm^2 and increased more or less linearly with the radiant exposure. With 10^4 pulses, an inactivation of 40% was observed even below 10 mJ/cm^2 . As multiple pulses were used, the degree of inactivation increased with the number of pulses. Therefore, a certain additivity of the effect was observed. Assuming all pulses act independently from each other, an exponential dependence of IA on the number of pulses is expected:

$$IA(N) = 1 - e^{-\alpha N}. \quad (7)$$

α gives the probability that a protein is damaged by one pulse. The measured increase of the inactivation with the number of pulses used for irradiation roughly shows this relationship.

The dependence of the inactivation on the radiant exposure is determined by the damage mechanism. Possible mechanisms are a thermal inactivation, mechanical destruction due to shock waves or evaporation of the water and photochemistry. In principle, a thermal inactivation of aP could be possible with in 10 ps. From inactivation experiments of aP solutions which were heated in a water bath, a frequency factor $A_0 = 1.85 \times 10^{23}$ and activation energy $E_a = 161 \text{ kJ/mol}$ were obtained as parameters for the Arrhenius equation, which describes the thermal damage rate k_{TD} at temperatures below 100°C :²³

$$k_{TD} = A_0 e^{-\frac{E_a}{RT}}. \quad (8)$$

R is the universal gas constant. If the Arrhenius equation is extrapolated to damage rates of 10^{11} 1/s , a temperature of 410°C is expected to be necessary for a thermal protein inactivation within 10 ps. According to the temperature calculations (Fig. 8), these temperatures are achieved at the surface with an radiant exposure of 4.5 mJ/cm^2 , whereas at a distance of 10 nm at least 90 mJ/cm^2 is necessary to reach 410°C . Even if the extrapolation of the Arrhenius equation into the picosecond range gave valid data, the extreme temperature gradient over the protein with an extend of 10 nm makes it very difficult to compare the results of the experiment with the Arrhenius theory.

In general, a sharp increase of the inactivation with increasing radiant exposure is expected for a thermal damage mechanism, since the damage rates depend exponentially on the temperature. This was not observed in the experiments. When the laser beam is scanned in the volume, the sharp increase of the inactivation is washed out, because,

although the average radiant exposure is quite homogeneous, the damage rates vary strongly in the sample, being highest at the maxima of the 16 beam position. If not the the surface temperature, but the temperature in some distance from the particle were responsible for the thermal protein damage, this would also lower the slope of the inactivation curves.²³

With the mathematical model from Sect. 3.2, a particle temperature of nearly 5000°C is calculated at a radiant exposure of 50 mJ/cm². This is well above the boiling point of gold. However, as gold melts at temperature of 1064°C, the absorbed energy is partly needed as latent heat for the melting process. With 15.5 kJ/mol, the latent heat is large enough to heat solid gold particles by 620 K. After melting, density, heat capacity, and thermal conductivity do not change very much.^{24,25} However, the complex index of refraction changes, and this will lower the absorption by 50%.²⁶ A simple estimation, which takes these effects into account, a particle temperature of 1700°C at 50 mJ/cm². These calculations do not account for the change of the properties of water with increasing temperature. As soon as water is evaporated, a gas bubble may be formed which insulates the particle from the surrounding water. In this case, the temperature could rise significantly since in the absence of heat conduction 1 mJ/cm² causes a temperature increase of 285 K instead of 100 K. This vapor bubble may also destroy the proteins or detach them from the surface of the particles.

It may also be possible that the aP lost its activity due to photochemical processes. Two different mechanisms are possible. Under irradiation with the picosecond pulses electrons, which oxidize the Amino acids in the aP, may be injected from the gold particles into water.²⁷ The second photochemical mechanism uses a direct 2-photon excitation of the protein. Aromatic amino acids decompose with a quantum efficiency η_{PD} of a few percent if excited with cw-irradiation at 254 nm.²⁸ For an irradiation with N the damage rate k_{PD} can be estimated with following equation:

$$k_{PD} = N \eta_{PD} \sigma_{2ph} \left(\frac{E}{\tau \frac{h c_0}{\lambda}} \right)^2. \quad (9)$$

Assuming a 2-photon absorption cross-section σ_{2ph} of 10⁵⁰ cm²s/photons,²⁹ a radiant exposure $E = 50$ mJ/cm², and a quantum efficiency for photodamage of 5%, the damage rate caused by the 2-photon absorption is $7 \cdot 10^7$ 1/s. This is approximately three orders of magnitude too slow in order to destroy the proteins during the pulse width τ which was 35 ps. A destruction of free proteins in solution is therefore not expected with these laser parameters. However, the electric field of the irradiation can be increased by several orders of magnitude at the surface of metallic particles. This effect causes increased Raman emission, known as the SERS effect. Also, an increase of the 2-photon absorption from molecules at the surface from metallic particles was observed.³⁰ Therefore, the proteins could also be destroyed by a "surface enhanced" 2-photon photochemistry.

In conclusion, protein inactivation is possible via nanoparticles and picosecond laser pulses. The confinement of the heat to the nanoabsorbers when irradiating with picosecond pulses suggests that a denaturation of single proteins in cells could be possible with this approach. However, the mechanism of protein inactivation which is part of present investigations is crucial for the precision of these nanoeffects.

ACKNOWLEDGMENTS

This work is supported by the German Science Foundation (DFG) under the grant Bi 321/3-1.

REFERENCES

1. N. Ponelies, J. Scheef, A. Harim, G. Leitz, and K. O. Greulich, "Laser micromanipulators for biotechnology and genome research," *J. Biotechnol.* **35**, pp. 109–120, 1994.
2. K. Schütze, I. Becker, K. F. Becker, S. Thalhammer, R. Stark, W. M. Heckl, M. Böhm, and H. Pösl, "Cut out or poke in — the key to the world of single genes: Laser micromanipulation as a valuable tool on the look-out for the origin of disease," *Genet. Anal.* **14**, pp. 1–8, 1997.
3. R. R. Anderson and J. A. Parrish, "Selective photothermolysis: Precise microsurgery by selective absorption of pulsed radiation," *Science* **220**, pp. 524–527, 1983.
4. C. Dierickx, M. B. Alora, and J. S. Dover, "A clinical overview of hair removal using lasers and light sources," *Dermatol. Clin.* **17**, pp. 357–666, 1999.

5. M. J. C. Van Gemert, A. J. Welch, J. W. Pickering, and T. O. T., "Laser treatment of port wine stains," in *Optical-Thermal Response of Laser-Irradiated Tissue*, A. J. Welch and M. J. C. Van Gemert, eds., pp. 789–829, Plenum Press, New York, 1995.
6. M. Landthaler, U. Hohenleutner, and T. A. el Raheem, "Laser therapy of childhood haemangiomas," *Br. J. Dermatol.* **133**, pp. 275–281, 1995.
7. J. Roider, F. Hillenkamp, T. Flotte, and R. Bringruber, "Microphotocoagulation: Selective effects of repetitive short laser pulses," *Proc. Natl. Acad. Sci. U.S.A.* **90**, pp. 8643–8647, 1993.
8. F. H. Johnson, H. Eyring, and B. J. Stover, *The theory of Rate Processes in biology and medicine*, Wiley, New York, 1974.
9. J. Pearce and S. Thomsen, "Rate process analysis of thermal damage," in *Optical-Thermal Response of Laser-Irradiated Tissue*, A. J. Welch and M. J. C. Van Gemert, eds., pp. 561–606, Plenum Press, New York, 1995.
10. G. A. Griess, M. F. Blankenstein, and G. G. Williford, "Ocular damage from multiple-pulse laser exposures," *Health Phys.* **39**, pp. 921–927, 1980.
11. W. T. Ham Jr., H. A. Mueller, M. L. Wolbarsht, and D. H. Sliney, "Evaluation of retinal exposures from repetitively pulsed and scanning lasers," *Health Phys.* **54**, pp. 337–344, 1988.
12. J. Roider, J. Traccoli, N. Michaud, T. Flotte, R. Anderson, and R. Birngruber, "Selektiver Gefäßverschuß durch repetierende kurze Laserpulse.," *Ophthalmologie* **91**, pp. 274–279, 1994.
13. G. Hüttmann and R. Birngruber, "On the possibility of high-precision photothermal microeffects and the measurement of fast thermal denaturation of proteins," *IEEE J. Select. Topics Quantum Electron.* **5**, pp. 954–962, 1999.
14. G. Jori and J. D. Spikes, "Photothermal sensitizers: possible use in tumor therapy," *J. Photochem. Photobiol. B.* **6**, pp. 93–101, 1990.
15. D. G. Jay, "Selective destruction of protein function by chromophore-assisted laser inactivation," *Proc. Natl. Acad. Sci. U.S.A.* **85**, pp. 5454–5458, 1988.
16. J. C. Liao, J. Roider, and D. G. Jay, "Chromophore-assisted laser inactivation of proteins is mediated by the photogeneration of free radicals," *Proc. Natl. Acad. Sci. U.S.A.* **91**, pp. 2659–2663, 1994.
17. M. Soncin, A. Buseti, F. Fusi, G. Jori, and M. A. Rodgers, "Irradiation of amelanotic melanoma cells with 532 nm high peak power pulsed laser radiation in the presence of the photothermal sensitizer cu(ii)-hematoporphyrin: a new approach to cell photoinactivation," *Photochem. Photobiol.* **69**, pp. 708–712, 1999.
18. A. Buseti, M. Soncin, E. Reddi, M. A. Rodgers, M. E. Kenney, and G. Jori, "Photothermal sensitization of amelanotic melanoma cells by Ni(II)-octabutoxy-naphthalocyanine," *J. Photochem. Photobiol. B.* **53**, pp. 103–109, 1999.
19. M. Saeed, D. Kim, and L. DiMauro, "Optimization and characterization of a high repetition rate, high intensity Nd:YLF regenerative amplifier," *Appl. Opt.* **29**, pp. 1752–1757, 1990.
20. H. C. van de Hulst, *Light scattering by small particles*, Dover Publications Inc., New York, 1981.
21. H. Goldenberg and C. J. Tranter, "Heat flow in an infinite medium heated by a sphere," *Brit. J. Appl. Phys.* **3**, pp. 296–298, 1952.
22. R. Roider and R. Birngruber, "Solution of the heat conduction equation," in *Optical-thermal response of laser-irradiated tissue*, J. Welch, A and M. J. C. van Gemert, eds., pp. 385–409, Plenum Press, New York, 1995.
23. J. Serbin, *Wechselwirkung von Gold-Protein-Konjugaten mit ultrakurzen Laserpulsen*. PhD thesis, Technical University München, 2000.
24. R. C. Weast, M. J. Astle, and W. H. Beyer, *CRC Handbook of Chemistry and Physics*, CRC Press, Boca Raton, Florida, 68 ed., 1987.
25. D. R. Lide and H. P. R. Frederikse, *CRC Handbook of Chemistry and Physics*, CRC Press, Boca Raton, New York, London, Tokyo, 76 ed., 1995.
26. U. Kreibig and M. Vollmer, *Optical Properties of Metal Clusters*, vol. 25 of *Springer Series in Material Science*, Springer, Berlin, Heidelberg, 1995.
27. J. Z. Zangh, B. A. Smith, A. E. Faulhaber, K. J. Andersen, and T. J. Rosales, "Femtosecond studies of colloidal metal nano-particles: Dependence of electronic energy relaxation on the liquid-solid interface and particle size.," in *Ultrafast Processes in Spectroscopy*, O. Svelto, ed., pp. 561–565, Plenum Press, New York, 1996.
28. D. N. Nikogosyan and G. Helmut, "Laser-induced photodecomposition of amino acids and peptides: Extrapolation to corneal collagen," *IEEE J. Select. Topics Quantum Electron.* **5**, pp. 1107–1115, 1999.

29. Y. W. Xu, J. R. Zhang, Y. M. Deng, L. K. Hui, S. P. Jiang, and S. H. Lian, "Fluorescence of proteins induced by two-photon absorption," *J. Photochem. Photobiol. B.* **1**, pp. 223–7, 1987.
30. G. Peleg, A. Lewis, O. Bouevitch, L. Loew, D. Parnas, and M. Linial, "Giant optical non-linearities from nanoparticle-enhanced molecular probes with potential for selectively imaging the structure and physiology of nanometric regions in cellular systems," *Bioimaging* **4**, pp. 215–224, 1996.